Applied Thermal Engineering 148 (2019) 557–567

Contents lists available at ScienceDirect

Applied Thermal Engineering

journal homepage: www.elsevier.com/locate/apthermeng

Research Paper

Numerical investigation of heat transfer and flow characteristics of laminar flow in a tube with center-tapered wavy-tape insert

Yunmin Liang, Peng Liu, Nianben Zheng, Feng Shan, Zhichun Liu*, Wei Liu

School of Energy and Power Engineering, Huazhong University of Science and Technology, Wuhan 430074, China

HIGHLIGHTS

- Center tapered wavy-tape insert is designed from bionics based on the movement of cuttlefish.
- It brings about significant effects on flow resistance reduction and better overall performance.
- Optimal situation of using the center tapered wavy-tape insert is studied.
- Two empirical formulas have been developed for *Nu* and f with an error band of ± 14%.

ARTICLE INFO

Keywords:
Center-tapered wavy-tape insert
Heat transfer augmentation
Flow resistance
Swirl flow
Bionic design

ABSTRACT

In this study, a new type of insert, named center-tapered wavy-tape insert, which is designed from bionics based on the movement of cuttlefish, is introduced. The thermo-hydraulic performance of laminar flow in a plain tube fitted with a center-tapered wavy-tape insert under constant heat flux conditions was investigated using numerical simulation. Further, the results were compared with the conventional wavy-tape insert. It was observed that the center-tapered wavy-tape inserts have a significant influence on the reduction of flow resistance and improvement of the overall performance for producing a similar flow structure and temperature field inside the tube with a small disturbance to the core area. The optimal conditions of use of the center-tapered wavy-tape insert were studied. The considered geometric parameter combinations of the model are provided herein. The best Nusselt number could be enhanced by 5.23–8.99 times and the best performance evaluation criterion could be improved to 2.62. Then, two empirical formulas were developed for predicting *Nu* and *f* with an error band of ± 14%. Finally, the numerical results were verified by the Stereo-PIV experiments.

1. Introduction

The design of a high-performance compact heat exchanger is an important solution for the problem of conversion and efficient use of energy. The techniques of heat transfer augmentation are widely used in this design process [1–4]. According to Bergles's [5] dissertation, these techniques are divided into three categories: passive, active, and compound enhancement techniques. Active techniques such as fluid vibration and mechanical aids require external power to enhance the convective heat transfer coefficient. Passive techniques require no external power to achieve this effect. Compound techniques involve more than one technique to obtain this augmentation. Owing to the characteristics of low energy consumption and easy implementation, passive techniques are more frequently utilized in practice. The application of tube insert is a typical example of a passive technique used to improve the efficiency of a heat exchanger [6].

Tube inserts are important heat transfer enhancement devices, especially in laminar and transition flows of high-viscosity fluids. Tube inserts are primarily used to generate swirl flow or vortex and modify the velocity distribution, which induces transverse fluid mixing between the core and near-wall regions while breaking the growth of the boundary layer simultaneously [7–10]. It is known that tube inserts produce two different effects—heat transfer enhancement and increase in flow resistance. Hence, numerous studies—both experimental and numerical—on tube inserts with excellent performance, specifically in terms of highly efficient heat transfer and low flow resistance, have been conducted by researchers worldwide.

Ibrahim [11] separately investigated the effect of spacer length and twist ratio on the thermo-hydraulic performance of a plain flat tube with helical screw-tape inserts using a test bench with a counter flow double-pipe heat exchanger. The results show that the flow resistance and heat transfer effect decrease with the increase in twist ratio and

* Corresponding author at: 1037 Luoyu Road, Hongshan District, Wuhan 430074, China.
E-mail address: zcliu@hust.edu.cn (Z. Liu).

https://doi.org/10.1016/j.applthermaleng.2018.11.090
Received 10 August 2017; Received in revised form 1 October 2018; Accepted 21 November 2018
Available online 22 November 2018
1359-4311/

Nomenclature

L	length of the tube, mm
D	diameter, mm
s	the clearance of the wavy tape, mm
w	the width of the wavy tape, mm
A	amplitude, mm
P	period, mm
u	flow velocity, m/s^{-1}
x_i	space coordinates in Cartesian system, m
T	temperature, K
ΔP	pressure drop, Pa
R	inner radius of the tube, m
r	radial distance, m
Re	Reynolds number
f	friction factor
Nu	Nusselt number
PEC	performance evaluation criterion
h	heat transfer coefficient, $W\,m^{-2}\,K^{-1}$
C_P	specific heat at constant pressure, $J\,kg^{-1}\,K^{-1}$
q	heat transfer rate per unit area, W/m^2
k	thermal conductivity of water, W/m K

Greek symbols

α	waveform factor, $\alpha = 2A/P \times 100\%$
β	period ratio, $\beta = P/D$
γ	amplitude ratio, $\gamma = 2A/D$
μ	dynamic viscosity, $kg\,m^{-1}\,s^{-1}$
ρ	fluid density, $kg\,m^{-3}$
δ	thickness of the wavy tape, mm

Subscripts

0	smooth tube
i, j	Cartesian coordinates
w	wall
m	mean
c	center

spacer length of the flat tube. Zhang et al. [12] illustrated the enhancement of heat transfer in a tube with helical screw-tape without core-rod inserts using a numerical method and employed the physical quantity synergy principle and minimal entropy generation principle for analysis. In their studies, they determined that there is an optimum width of helical screw-tape relative to the fixed tube diameter to obtain a good overall performance. García et al. [13] experimentally studied the heat transfer and flow characteristics of a circular tube with wire coil inserts in laminar, transition, and turbulent flows at different Prandtl numbers. Akhavan-Behabadi et al. [14] investigated the pressure drop and heat transfer augmentation of a horizontal tube with coiled wire inserts.

Eiamsa-ard et al. [15,16] experimentally investigated the heat transfer and flow characteristics of a circular tube with full-length typical twisted tape inserts and its variants, such as regularly spaced twisted tapes and alternate clockwise and counterclockwise twisted tapes. The correlations of the Nusselt number and the friction factor were proposed, and the predictive values were within ± 15% of the experimental results. Guo [17] and Li [18] numerically investigated the heat transfer and friction factor characteristics of a center-cleared twisted tape and centrally hollow narrow twisted tapes in a laminar region, respectively. The both results demonstrated that a suitable central clearance could enhance the heat transfer and reduce the flow resistance simultaneously. Syam Sundar [19] conducted experiments with magnetic nanofluid as the working fluid in a tube fitted with twisted tape to study the convective heat transfer and friction factor characteristics in a turbulent region.

In addition to the common inserts mentioned above, new tube insert configurations with promising thermo-hydraulic performances have been reported. Zheng and Liu [20–22] investigated a rod-type vortex generator arranged in the surrounding called vortex rods, arranged in the center called central slant rods. The results indicate that both these vortex generators exhibit a promising performance for the heat transfer enhancement of laminar flow. Li et al. [23] investigated the heat transfer and flow characteristics of a tube with drainage inserts in turbulent flow and developed the correlations of the Nusselt number and friction factor. Tu et al. [24] experimentally reported the effects of particle size and particle shape of the porous media inserts on the heat transfer and friction factor characteristics. Furthermore, Tu et al. [25] numerically investigated the thermo-hydraulic performance of a circular tube with pipe inserts.

By investigating the mechanism of heat transfer augmentation by different types of tube inserts, it can be observed that a longitudinal swirl flow with single vortex or multiple vortexes appears in the flow field leading to the enhancement of heat transfer with relatively moderate flow resistance. Liu et al. [26–28] illustrated this mechanism using theoretical approaches, such as the minimum heat consumption principle, minimum power consumption principle, and minimum entransy dissipation, separately. Based on this mechanism, Zhu et al. [29] introduced the heat transfer augmentation and flow characteristics of a straight tube with novel wavy-tape inserts, which are desired longitudinal vortex generators. The parametric studies demonstrated that the tape amplitudes had a distinct influence on the thermo-hydraulic performance. For the same Reynolds number, the larger the tape amplitudes, the higher the Nusselt number and the friction factor. However, excessive flow resistance limits the overall performance. The bionic method has a wide range of applications for the reduction of flow resistance [30–33]. Considering the good mobility of cuttlefish, the movement of their fins was observed and investigated [34]. It was observed that it presents a special wave structure. The amplitude of the wave structure gradually increased from the middle to the two sides. Inspired by this finding, we designed a new type of insert—a center-tapered wavy-tape insert—as shown in Fig. 1, to reduce the flow resistance and improve the overall performance.

In the present study, the thermo-hydraulic performances of laminar flow of a tube with center-tapered wavy-tape inserts are investigated. In this tube, water is the working fluid. Compared with the conventional wavy-tape inserts, the center-tapered wavy-tape inserts have a significant effect on the reduction of flow resistance and improvement of the overall performance. Further, the investigations of two main dimensionless numbers related to the degree of the waveform and the size of the insert relative to the tube diameter are carried out to determine

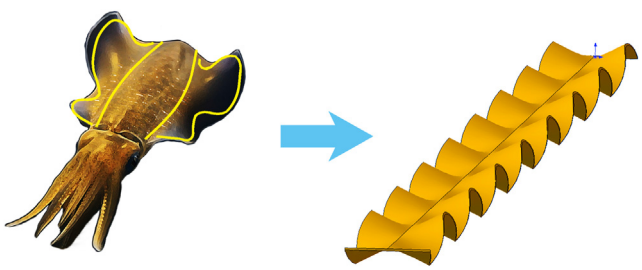

Fig. 1. Cuttlefish fins and center-tapered wavy-tape inserts.

the optimal conditions of use of the center-tapered wavy-tape inserts.

2. Physical model

The layout and configuration of the center-tapered wavy-tape inserts and the conventional wavy-tape inserts are illustrated in Fig. 2. As shown in the figure, both the wavy-tape inserts were fitted into the center of the tube. The length (L) and diameter (D) of the tube were 500 mm and 20 mm, respectively. The outer contour of the inserts was arcuate for a better fit to the shape of the tube wall. The clearance (s) between the inserts and tube wall was 1 mm. The thickness (δ) and width (w) of the inserts were 0.5 mm and 18 mm, respectively. The tape waviness of the two wavy-tape inserts presented a sinusoidal shape. The amplitude (A) of the center-tapered wavy-tape inserts gradually increased from the middle to the two sides, and the amplitude was 0 at the middle. The amplitude of the conventional wavy-tape inserts did not change from the middle to the two sides. Both the period (P) and amplitude of the center-tapered wavy-tape inserts were variable and the geometric parameter combinations of the model are listed in Table 2.

3. Mathematical model and numerical method

3.1. Governing equations

The problem under consideration was assumed to be three-dimensional, laminar, and steady. The physical properties of the fluid were assumed to be constant. The flow was assumed to be incompressible and the influences of the body forces, thermal radiation, and viscous dissipation were not considered. Furthermore, the vibration and deformation of the wavy-tape inserts were neglected. The governing equations of continuity, momentum, and energy are expressed as follows:

Continuity equation:
$$\frac{\partial u_i}{\partial x_i} = 0 \tag{1}$$

Momentum equation:
$$\rho u_i \frac{\partial u_j}{\partial x_i} = -\frac{\partial p}{\partial x_i} + \frac{\partial}{\partial x_i}\left(\mu \frac{\partial u_j}{\partial x_i}\right) \tag{2}$$

Energy equation:
$$\rho c_p \left(u_i \frac{\partial T}{\partial x_i}\right) = k\left(\frac{\partial^2 T}{\partial x_i^2}\right) \tag{3}$$

3.2. Boundary conditions

In the present work, the Reynolds number in the tube ranged from 600 to 1800, and the tube wall was under a constant heat flux condition. At the tube inlet, fully developed flow and temperature boundary conditions were applied, which are defined as follows:

Inlet temperature condition:
$$T = T_c + \frac{qR}{k}\left[\left(\frac{r}{R}\right)^2 - \frac{1}{4}\left(\frac{r}{R}\right)^2\right] \tag{4}$$

Inlet velocity condition:
$$u = u_c\left(1 - \frac{r^2}{R^2}\right) \tag{5}$$

where T_c and u_c are the temperature and velocity at the center of the cross-section of the tube inlet, respectively.

The outflow condition was used at the tube outlet. Non-slip conditions were imposed on the tube walls and surfaces of the inserts.

3.3. Data processing

The Reynolds number (Re), heat transfer coefficient (h), Nusselt number (Nu), and Fanning friction coefficient (f) are defined as follows:

$$Re = \frac{\rho u D}{\mu} \tag{6}$$

$$h = \frac{q}{T_w - T_m} \tag{7}$$

where T_w and T_m are the temperature on the tube wall and fluid bulk temperature inside the tube, respectively.

$$T_w = \frac{1}{A}\int_0^A T dA \tag{8}$$

$$T_m = \frac{\int_0^R uTrdr}{\int_0^R urdr} \tag{9}$$

$$Nu = \frac{hD}{k} \tag{10}$$

$$f = \frac{\Delta P}{(\frac{1}{2}\rho u^2)(\frac{L}{D})} \tag{11}$$

The performance evaluation criterion (PEC) proposed by Webb [35] is defined as follows:

$$PEC = \frac{Nu/Nu_0}{(f/f_0)^{1/3}} \tag{12}$$

where Nu_0 and f_0 are the Nusselt number and Fanning friction factor of the plain tube, respectively.

3.4. Numerical method

The commercial CFD software FLUENT 14.0 was chosen for the present investigation and the finite volume method was used for the numerical computation. The SIMPLE algorithm was selected to achieve pressure–velocity coupling. The discretization was carried out with the second-order upwind scheme. Further, the solutions were considered to have converged when the residuals for the continuity, momentum, and energy equations were less than 10^{-6}.

3.5. Grid system and model validation

The sketch of the mesh of the center-tapered wavy-tape inserts is illustrated in Fig. 3. The mesh was denser near the tube wall and insert surface to better simulate the boundary layer flow. Grid-independent test was conducted by a Grid Convergence Index (GCI) method suggested by Roache [36]. Three successive refined grids for the center-tapered wavy-tape inserts were conducted to ensure the accuracy of the

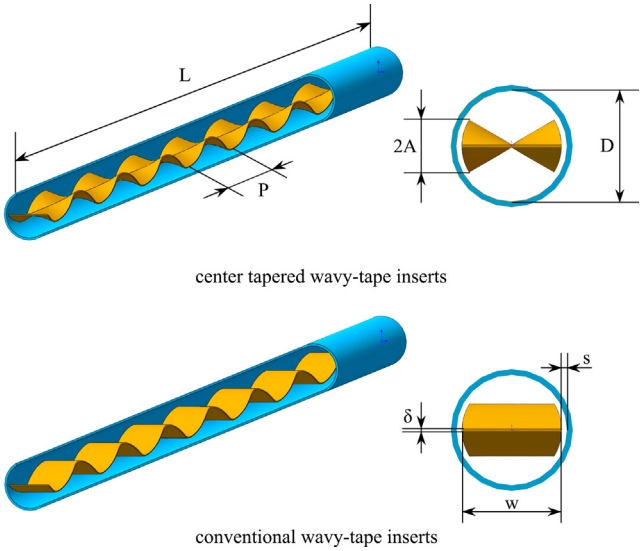

Fig. 2. Layout and configuration of the center-tapered wavy-tape inserts and the conventional wavy-tape inserts.

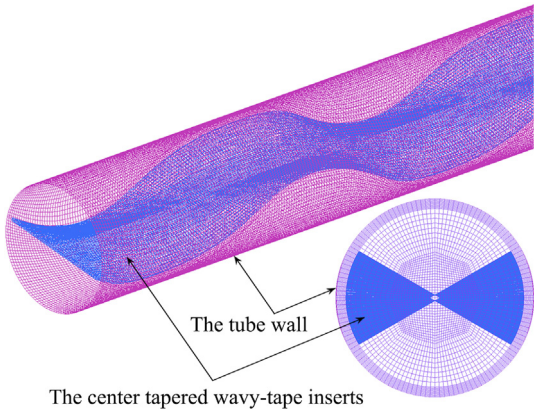

Fig. 3. Mesh of the center-tapered wavy-tape inserts.

Table 1
Grid Convergence Index (GCI) for different grids.

Cell numbers	*Nu*	GCI(*Nu*)	*f*	GCI(*f*)
12,68,410	11.9008	1.37%	0.26654	6.32%
41,02,064	11.9718	0.63%	0.27386	2.89%
75,88,817	11.9736	0.33%	0.27589	1.91%

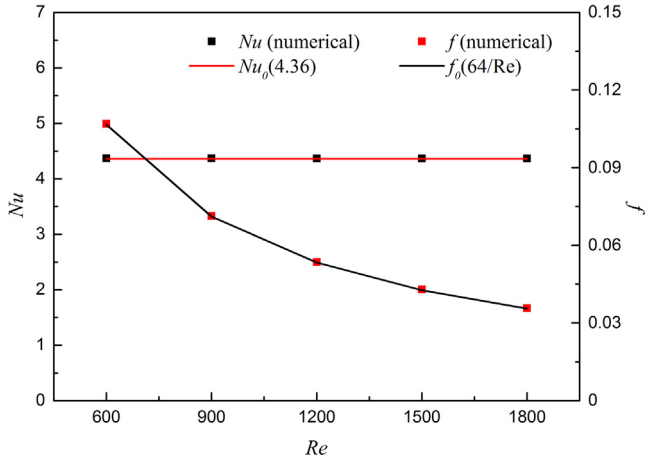

Fig. 4. Verification results for the Nusselt number and friction factor of the smooth tube.

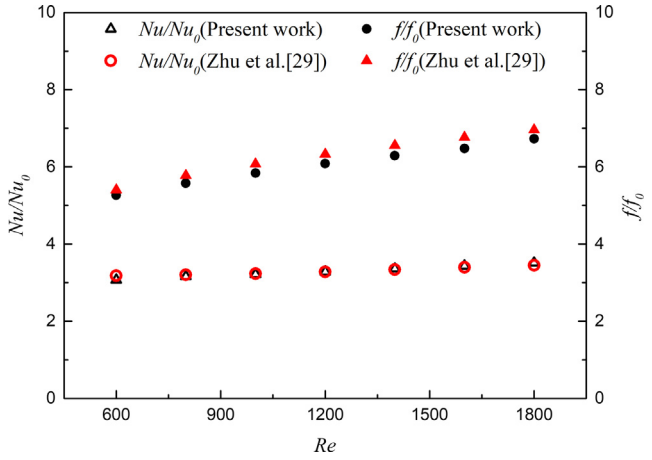

Fig. 5. Comparisons between present work and Zhu's work [29].

Table 2
Geometric parameter combinations of the model.

β = 2 (P = 40 mm)			β = 2.5 (P = 50 mm)			β = 3 (P = 60 mm)		
α	A (mm)	γ	A	A (mm)	γ	α	A (mm)	γ
9%	1.8	0.18	9%	2.25	0.225	9%	2.7	0.27
12%	2.4	0.24	12%	3	0.3	12%	3.6	0.36
15%	3	0.3	15%	3.75	0.375	15%	4.5	0.45
18%	3.6	0.36	18%	4.5	0.45	18%	5.4	0.54
21%	4.2	0.42	21%	5.25	0.525	21%	6.3	0.63
24%	4.8	0.48	24%	6	0.6	24%	7.2	0.72
27%	5.4	0.54	27%	6.75	0.675	27%	8.1	0.81

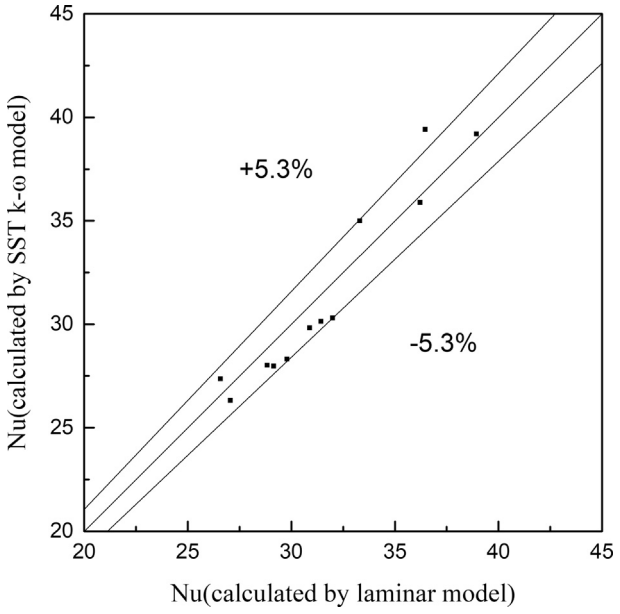

Fig. 6. Deviations of *Nu* calculated by laminar model and SST k-ω model.

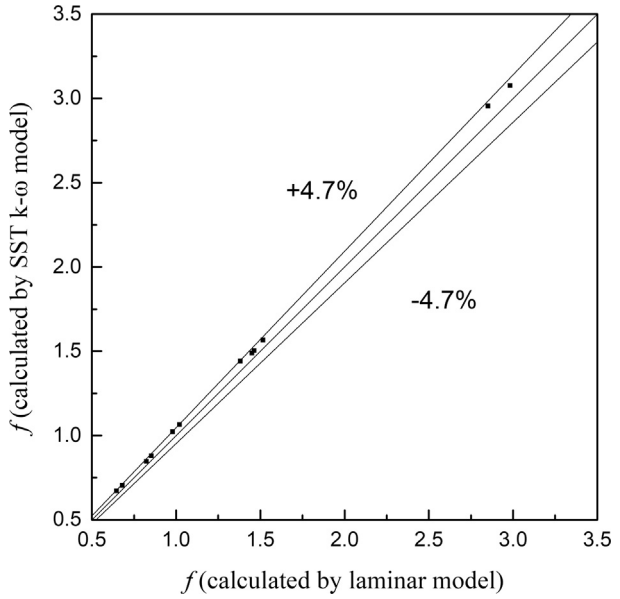

Fig. 7. Deviations of fiction factor calculated by laminar model and SST k-ω model.

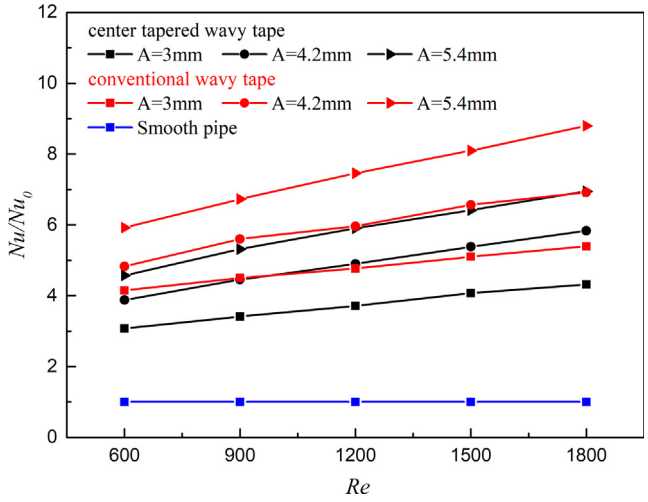

Fig. 8. Comparisons of the heat transfer enhancement ratio Nu/Nu_0 between a smooth tube with the center-tapered wavy-tape inserts (P = 40 mm, A = 3, 4.2, 5.4 mm) and a smooth tube with the conventional wavy-tape inserts (P = 40 mm, A = 3, 4.2, 5.4 mm) for the same *Re*.

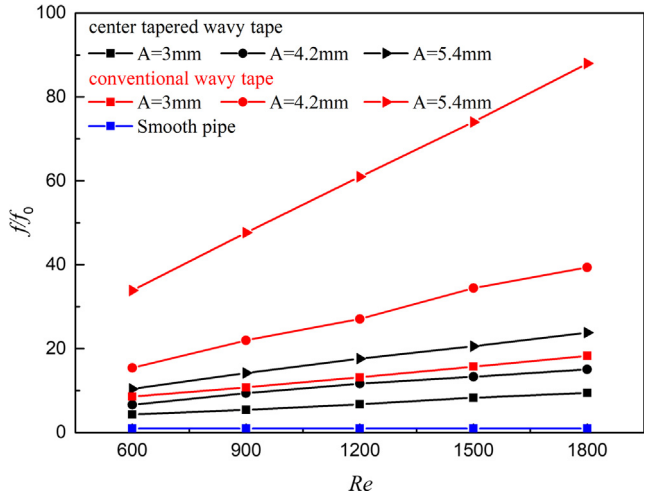

Fig. 9. Comparisons of the friction factor enhancement ratio f/f_0 between a smooth tube with the center-tapered wavy-tape inserts (P = 40 mm, A = 3, 4.2, 5.4 mm) and a smooth tube with the conventional wavy-tape inserts (P = 40 mm, A = 3, 4.2, 5.4 mm) for the same *Re*.

numerical solutions. The amplitude and period of the model were 2.7 mm and 60 mm, respectively. Furthermore, the numerical simulation was performed under a Reynolds number of 1200. As list in Table 1, the *Nu* and *f* values were obtained by the three grid systems and the Grid Convergence Index (GCI) was calculated for different mesh resolutions. Based on the results of this Grid-independent test and weighing computational costs, the grid system with 41,02,064 elements was adopted for the subsequent simulations.

In order to validate the accuracy of the numerical model, the Nusselt number (*Nu*) and friction factor (*f*) of the smooth tube were compared with the theoretical values, as shown in Fig. 4. The results demonstrate that the numerical solutions were consistent with the theoretical values. The deviations were limited to ± 1%. The results for a configuration with a conventional wavy-tape insert in Zhu's work [29] were used to further validate the accuracy of the numerical method. The comparisons of heat transfer enhancement ratio Nu/Nu_0 and friction factor enhancement ratio f/f_0 are illustrated in Fig. 5. As shown in the figure, the results were consistent with Zhu's work [29]. The maximum deviations were within 3.5% for Nu/Nu_0 and 4.5% for f/f_0. Considering

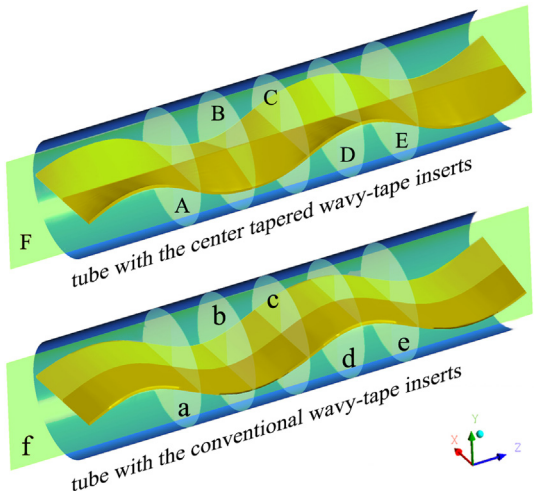

Fig. 10. Center symmetry plane and five different transverse planes in the entry sections of a tube with the center-tapered wavy-tape inserts and a tube with the conventional wavy-tape inserts.

some cases in this study may promote the transition of laminar flow, the SST k-ω turbulence model [37] which incorporates modifications for low-Reynolds number effects was applied in those cases to verify that whether the laminar flow model is still applicable. As listed in Table 2, the cases with the two largest amplitudes in each of the three periods were numerical investigated again at *Re* number is 1500 and 1800. The deviations of *Nu* and friction factor calculated by laminar model and SST k-ω model are shown in Figs. 6 and 7, respectively. The figures indicate that most deviations of *Nu* are within 5.3% except that only one point is 8.1%, and all deviations of friction factor are within 4.7%. In our work, the degree of turbulence caused by the center-tapered wavy-tape inserts was very slight, and the results calculated by the two physical models were similar. To carry out an investigation in a unified and reasonable manner, the problem investigated in our work was reasonably tackled as a laminar duct flow. Therefore, the numerical simulation method is reliable.

4. Results and discussion

4.1. Comparisons of thermal and hydraulic performances

In order to illustrate the effects of the novel design of the inserts, the thermal and hydraulic performances of a smooth tube with center-tapered wavy-tape inserts were compared with those of a smooth tube with conventional wavy-tape inserts under the same Reynolds number conditions and geometric parameters. The period of the two wavy-tape inserts was fixed as 40 mm, and the amplitudes were set as 3 mm, 4.2 mm, and 5.4 mm respectively.

The comparisons of heat transfer enhancement ratio Nu/Nu_0 and friction factor enhancement ratio f/f_0 between smooth tubes with center-tapered wavy-tape inserts and conventional wavy-tape inserts under the same Reynolds number conditions are illustrated in Figs. 8 and 9, respectively. As shown in the figure, *Nu* of a smooth tube with the conventional wavy-tape inserts was enhanced by 4.15–8.80 times in the considered *Re* range, whereas that of a smooth tube with the center-tapered wavy-tape inserts was enhanced by 3.07–6.95 times in the considered *Re* range. Further, Nu/Nu_0 increased as *Re* increased. Both the wavy-tape inserts had a significant effect on the heat transfer enhancement compared to the smooth tube without them. Furthermore, Nu/Nu_0 increased with the increase in the amplitudes for both the center-tapered wavy-tape inserts and conventional wavy-tape inserts. In other words, larger amplitudes were required to achieve a stronger heat transfer effect. The results also show that Nu/Nu_0 of a smooth tube with

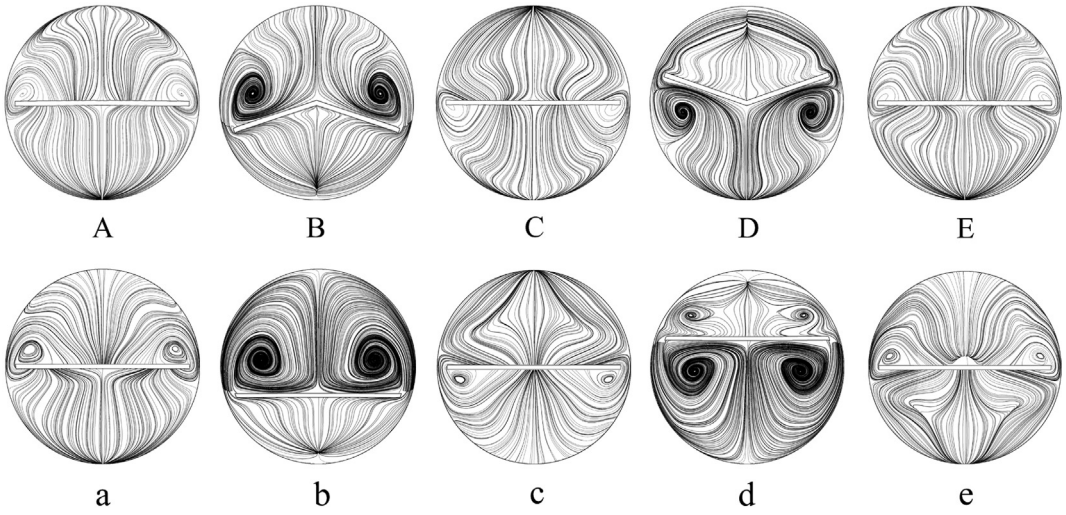

Fig. 11. Streamlines in five different transverse planes of a tube with the center-tapered wavy-tape inserts and a tube with the conventional wavy-tape inserts at Re = 600.

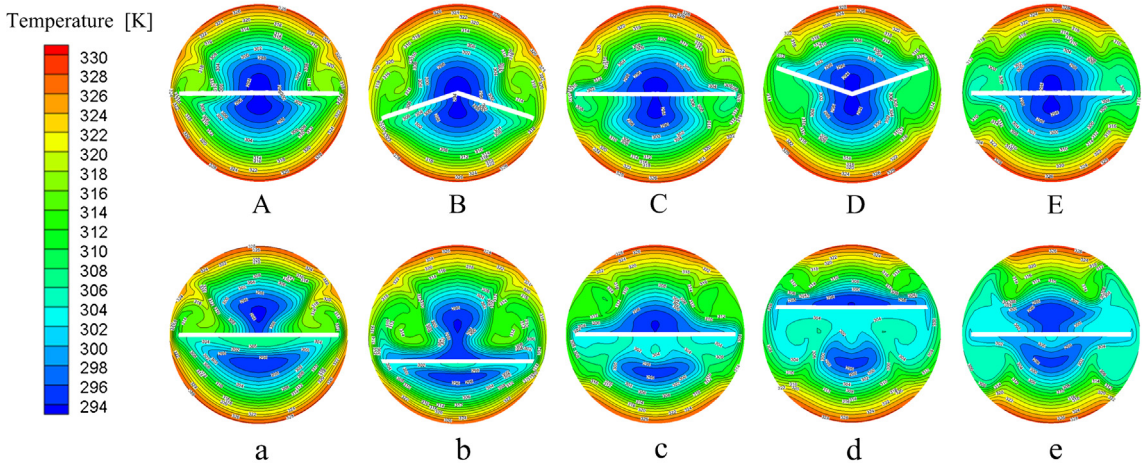

Fig. 12. Contour plots of the temperature field in five different transverse planes of a tube with the center-tapered wavy-tape inserts and a tube with the conventional wavy-tape inserts at Re = 600.

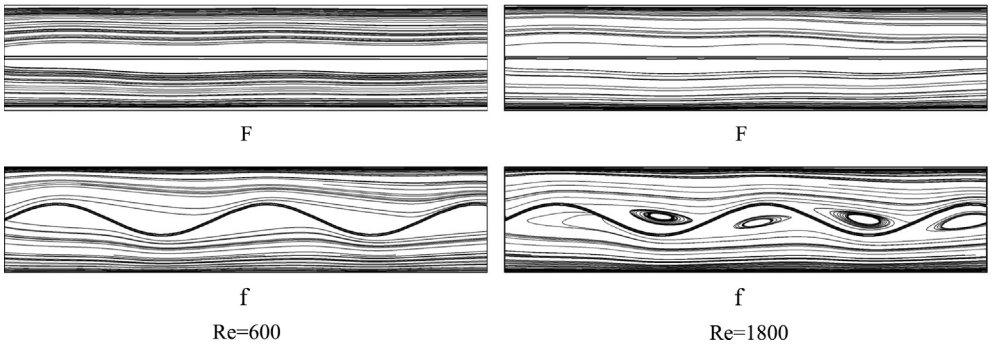

Fig. 13. Streamlines in the center symmetry plane of a tube with the center-tapered wavy-tape inserts and a tube with the conventional wavy-tape inserts at Re = 600 and Re = 1800.

the center-tapered wavy-tape inserts was lower than that of a smooth tube with the conventional wavy-tape inserts with the same amplitude. The enhanced heat transfer effects caused by the structural improvement of the center-tapered wavy-tape inserts was 15.6–25.9% less than the conventional wavy-tape inserts.

Fig. 9 indicates that the two wavy-tape inserts result in an increase in the flow resistance compared to the smooth tube without them. The value of f of a smooth tube with the conventional wavy-tape inserts was enhanced by 8.59–87.98 times in the considered Re range. The value of f of a smooth tube with the center-tapered wavy-tape inserts was enhanced by 4.34–23.81 times in the considered Re range. When Re increased, f/f_0 of the smooth tube with the conventional wavy-tape inserts increased faster than the smooth tube with the center-tapered wavy-tape inserts with the same amplitude. Furthermore, this tendency was more obvious as the amplitudes became larger. Under the same Re conditions, the flow resistance caused by the conventional wavy-tape

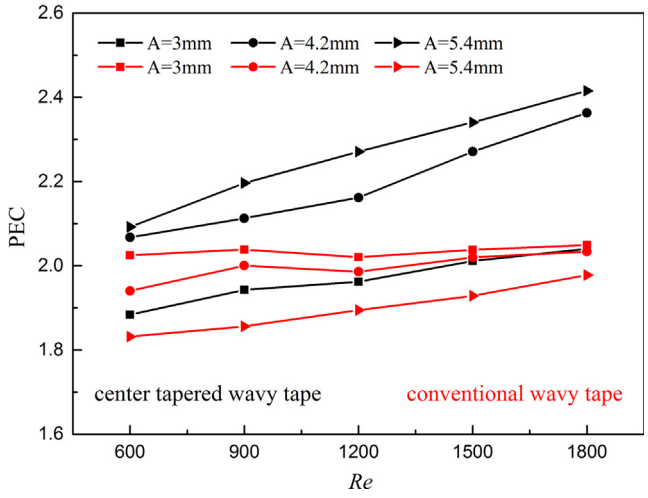

Fig. 14. Comparisons of the overall enhancement ratio PEC between a smooth tube with the center tapered wavy-tape inserts (P = 40 mm, A = 3, 4.2, 5.4 mm) and a smooth tube with the conventional wavy-tape inserts (P = 40 mm, A = 3, 4.2, 5.4 mm) for the same *Re*.

inserts was much higher than that caused by the center-tapered wavy-tape inserts with the same amplitudes. Specifically, the former was 93.4–269.5% more than the latter.

In order to analyze the mechanism of the different thermo-hydraulic performances caused by the two types of wavy-tape inserts, the flow structure and temperature distribution inside the tape-inserted tube were investigated, and the amplitude of the wavy-tape was 3 mm. The center symmetry plane and five different transverse planes in the tube entry section were observed. The viewing surfaces are shown in Fig. 10, and the transverse planes exactly covered one period of the wavy-tape. The longitudinal flow streamlines in five different transverse planes of a tube with the center-tapered wavy-tape inserts and a tube with the conventional wavy-tape inserts at $Re = 600$ are plotted in Fig. 11. It can be observed that, owing to the disturbance of the wavy-tapes, pairs of counter-rotating vortices were generated, especially in the trough or crest of the wavy-tapes; the magnitude of the vortices and the region influenced by the vortex cores increased gradually. As the stream reached the end of a whole wavy-period, the flow structures were similar to that at the beginning of the wavy-period. Further, the rheological process of the flow repeated the previous cycle with small changes in the position and magnitude of the vortices for the subsequent period of wavy-tapes. The contour plots of the temperature field in these transverse planes of the tube inserted with different tapes at $Re = 600$ are plotted in Fig. 12. Contacting the flow streamlines in the transverse planes, the vortices formed a transverse fluid mixture between cold water in the core region and hot water in the near-wall region; simultaneously, the thermal boundary layers were broken under the disturbance of the fluid. Compared with the temperature field at the beginning of the wavy period, the degree of temperature uniformity was improved at the end of a whole wavy period. Consequently, the heat transfer was enhanced. However, owing to the constraints of the different shapes of the two wavy-tape inserts, the thermal and hydraulic performances exhibited slight differences. As the amplitude of the center-tapered wavy-tape inserts gradually increased from the middle to the two sides, the disturbance in the core region induced by the center-tapered wavy-tape inserts was not as strong as that induced by the conventional wavy-tape inserts. From Fig. 11, it is evident that, at position-D, the streamlines above the tape were curved, but no vortices were formed; at position-d, a pair of counter-rotating vortices was generated above the tape, and the vortex cores generated by the center-tapered wavy-tape inserts were smaller than the others. Furthermore, comparing the temperature distribution between position-A to position-E and position-a to position-e in Fig. 12, the temperature field in the core region inside the tube with the center-tapered wavy-tape inserts exhibited no obvious change, but the other field exhibited a significant change under the disturbance caused by the conventional wavy-tape inserts. After the fluids were mixed for a whole wavy period, position-e had better temperature uniformity than position-E. For a comprehensive study, the streamlines in the center symmetry plane of a tube inserted with different tapes at $Re = 600$ and $Re = 1800$ are plotted in Fig. 13. When $Re = 600$, the streamlines at position-F were almost straight lines, but at position-f, the streamlines were forced to change the direction of flow owing to the obstruction by the conventional wavy-tape inserts. As the *Re* increased to 1800, the streamlines were still at position-F, but the backflows were formed at position-f, which resulted in a considerable loss of momentum. Hence, the flow resistances caused by the conventional wavy-tape inserts were much larger than those caused by the center-tapered wavy-tape inserts. In general, both the types of wavy-tape inserts produced a similar flow structure and temperature field inside the tube, and hence, the heat transfer enhancement caused by the center-tapered wavy-tape inserts and the conventional wavy-tape inserts was similar. However, owing to the lack of disturbance to the core area, the swirl flow and transverse vortices generated by the center-tapered wavy-tape inserts were not forceful, and the heat transfer enhancement of the center-tapered wavy-tape inserts were not as good as that of the conventional wavy-tape inserts, but the flow resistances caused by the former were much less than the latter.

4.2. Overall thermo-hydraulic performance evaluation

The comparisons of the PEC of smooth tubes with the center-tapered wavy-tape inserts and the conventional wavy-tape inserts under the same Reynolds number conditions are illustrated in Fig. 14. It was observed that, when the amplitude was small, the overall thermo-hydraulic performance of the smooth tube with the conventional wavy-tape inserts was only slightly better. As the amplitudes increased, the heat transfer was enhanced, but excessive flow resistances were formed by the conventional wavy-tape inserts, resulting in a decrease in PEC.

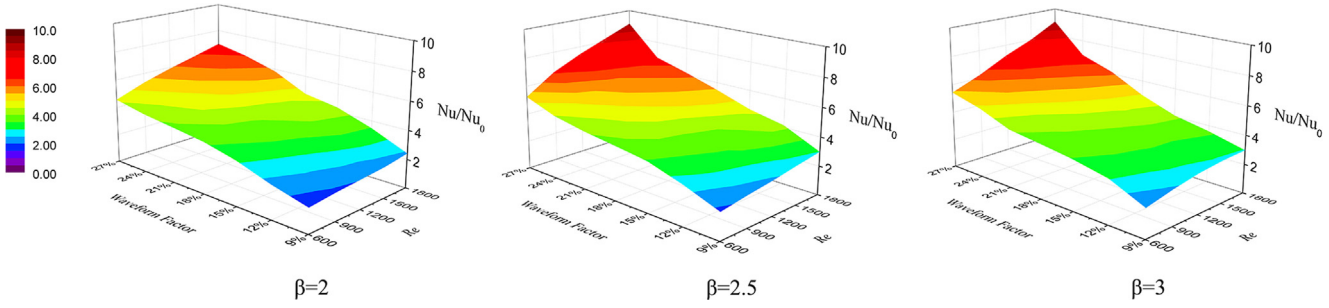

Fig. 15. Variation of the heat transfer enhancement ratio Nu/Nu_0 with different combinations of waveform factor and period ratio for a smooth tube with the center-tapered wavy-tape inserts.

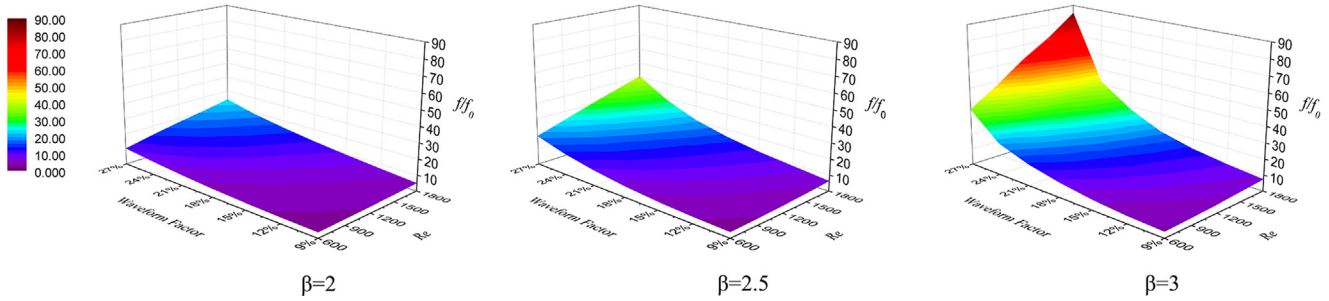

Fig. 16. Variation of the friction factor enhancement ratio f/f_0 with different combinations of waveform factor and period ratio for a smooth tube with the center-tapered wavy-tape inserts.

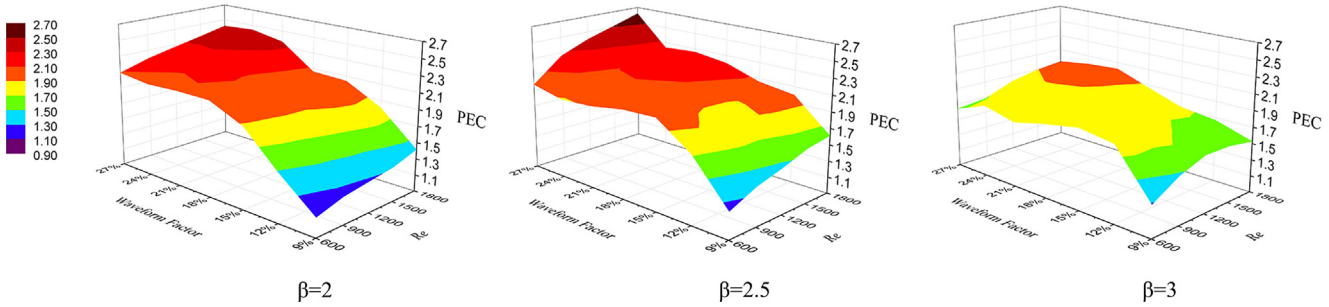

Fig. 17. Variation of the overall enhancement ratio PEC with different combinations of waveform factor and period ratio for a smooth tube with the center-tapered wavy-tape inserts.

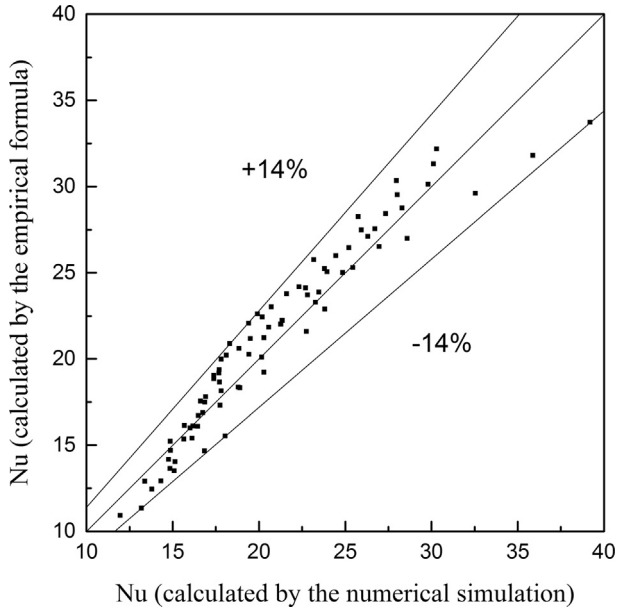

Fig. 18. Deviations of *Nu* calculated between the empirical formula and numerical simulation.

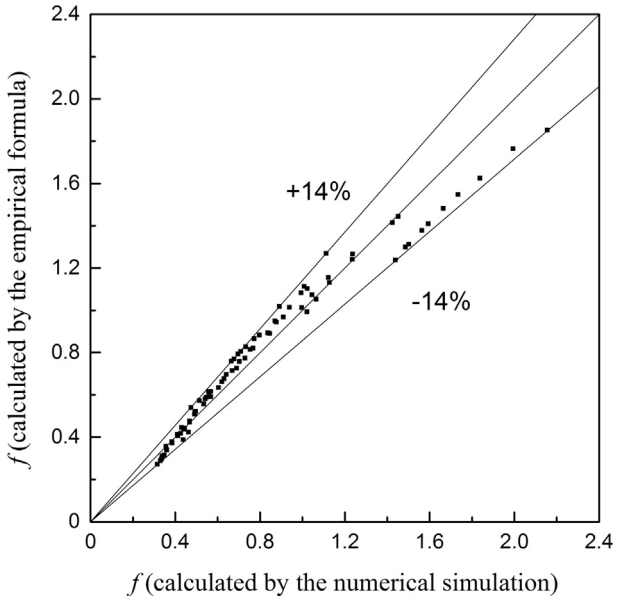

Fig. 19. Deviations of *f* calculated between the empirical formula and numerical simulation.

However, this tendency was opposite in the tube with the center-tapered wavy-tape inserts, wherein the PEC increased with an increase in the amplitudes. When the amplitude was 5.4 mm, the best PEC of the conventional wavy-tape inserts was 1.98 at Re = 1800, but the corresponding value of the center-tapered wavy-tape inserts was 2.42. The performance improvement was 22%. Therefore, in applications requiring higher heat transfer and lower flow resistance, the center-tapered wavy-tape inserts are a better choice than the conventional wavy-tape inserts.

4.3. Parametric studies

A different research perspective on the geometric parameters of the model is introduced in this section. In order to determine the optimal conditions of use of the center-tapered wavy-tape inserts, wavy tapes with seven wave shapes, each having three sizes relative to the tube diameter, were tested. Further, two main dimensionless numbers were studied. The waveform factor ($\alpha = 2A/P \times 100\%$), which indicates the degree of undulation of the wavy tapes, was used to determine the wave shape of the center-tapered wavy-tape inserts, and α was set as 9%, 12%, 15%, 18%, 21%, 24%, and 27%. The period ratio ($\beta = P/D$), which indicates the size of the wavy tapes relative to the tube diameter,

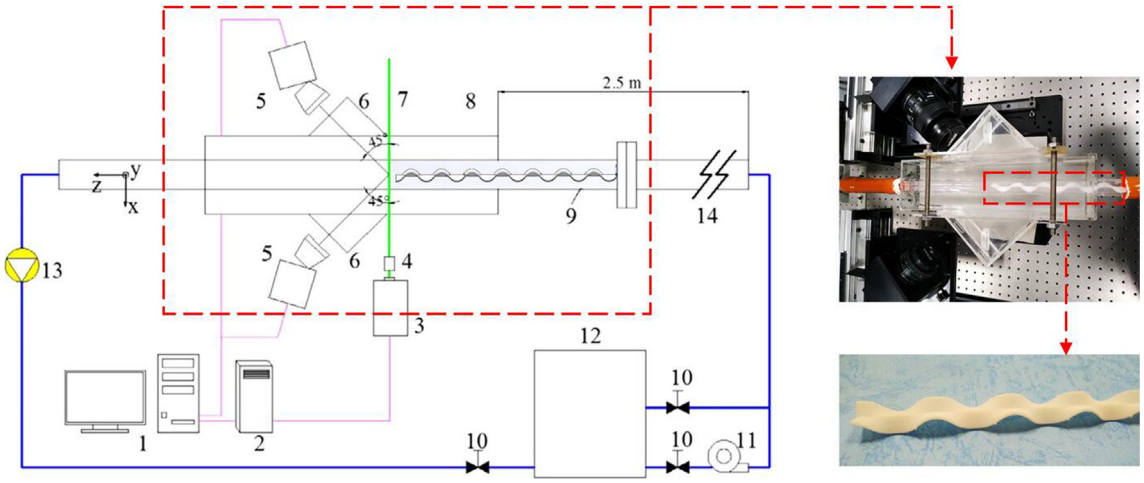

Fig. 20. Schematic of the Stereo-PIV system. 1. Computer, 2. PIV supply unit, 3. Laser, 4. Lenses, 5. CCD cameras, 6. Water prism, 7. Light sheet, 8. Test section, 9. Inserts, 10. Control valves, 11. Water pump, 12. Water tank, 13. Electromagnetic flowmeter, 14. Upstream tube.

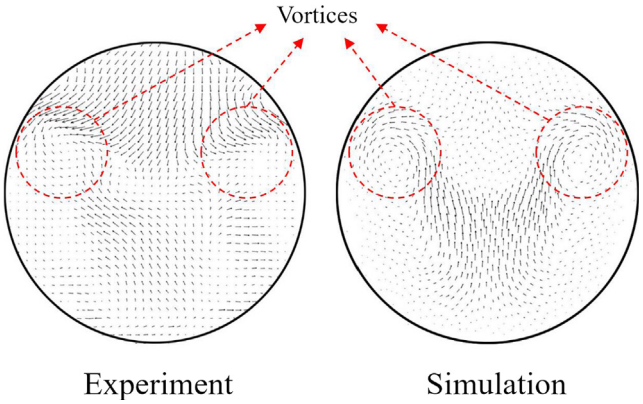

Fig. 21. Schematic diagram of velocity vectors in a circular tube with the center-tapered wavy-tape inserts tested by a PIV experiment at Re = 600.

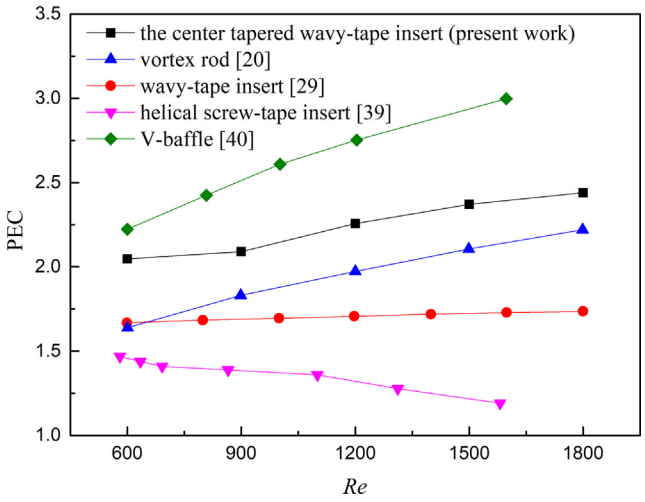

Fig. 23. Comparisons with previous work.

was used to determine the size of the center-tapered wavy-tape inserts, and β was set as 2, 2.5, 3. The waveform factor and period ratio combinations of the model and the corresponding amplitudes and period combinations are listed in Table 2.

The variation of the heat transfer enhancement ratio Nu/Nu_0, friction factor enhancement ratio f/f_0, and overall enhancement ratio PEC with different combinations of waveform factor and period ratio for a smooth tube with the center-tapered wavy-tape inserts are illustrated in Figs. 15–17 respectively. It can be observed that, under the same period ratio, Nu/Nu_0 and f/f_0 increased with the increases in the waveform factor and Re. The undulation of the wavy tapes was more intense, the heat transfer effect was better, and the flow resistance was larger. When the waveform factor was fixed, changing the relative size of the center-

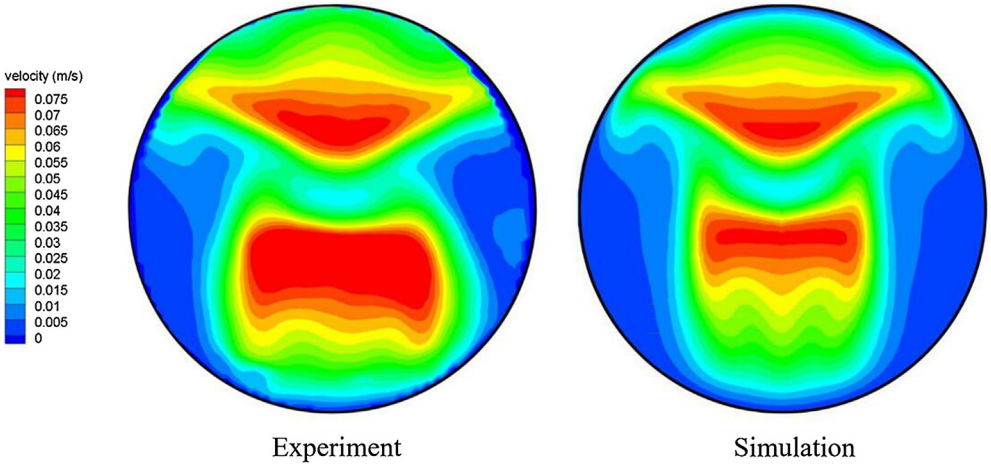

Fig. 22. Schematic diagram of velocity magnitudes in a circular tube with the center-tapered wavy-tape inserts tested by a PIV experiment at Re = 600.

tapered wavy-tape inserts influenced the thermo-hydraulic performance. In order to compare the cases of β = 2 and β = 2.5, increasing the period ratio resulted in a significant augmentation of heat transfer, and hence, the flow resistance increased inevitably. However, to compare the cases of β = 2.5 and β = 3, the heat transfer enhancement produced by increasing the period ratio was not obvious; on the contrary, continuing to increase this value resulted in a significant flow resistance. As shown in Fig. 17, under the same *Re*, when the waveform factor was larger than 15%, the PEC of the wavy-tapes with β = 2 or β = 2.5 were similar and higher than that of the wavy-tape with β = 3, but when the waveform factor was lower than 15%, the overall thermo-hydraulic performance was not good, irrespective of how large the relative size was. Furthermore, the wavy-tape with intense undulation and large relative size was unavailable for the significant flow resistance. In order to optimize the combinations of waveform factor and period ratio of the wavy-tapes, the dimensionless number amplitude ratio (γ = 2A/D) was defined, which indicates the extent of space filled in the tube. In order to analyze all the cases tested in this study, as it can be observed that a small amplitude ratio results in low heat transfer enhancement but a large amplitude ratio produces a significant flow resistance, the range of γ worth considering may be from 0.3 to 0.7. Over this amplitude ratio range, the center-tapered wavy-tape inserts with a high waveform factor and a suitable period ratio of approximately 2–2.5 can realize strong heat transfer enhancement and high overall thermo-hydraulic performance. The specific geometric parameters can be selected according to the actual engineering requirements.

4.4. Empirical formula

For practical use of the empirical formulas, only those data of cases with the amplitude ratio ranging from 0.3 to 0.7 were considered, and the empirical formulas are given as follows:

$$f = 41.4623 \times \beta^{1.477} \times Re^{-0.32277} \times \alpha^{1.8684} \quad (13)$$

$$Nu = 8.7804 \times \beta^{0.20995} \times Re^{0.32077} \times \alpha^{0.95572} \quad (14)$$

In Figs. 18 and 19, the maximum deviation of *Nu* and *f* between the numerical simulation and empirical formulas is 14%.

4.5. PIV testing verification

The analyses above indicate that pairs of counter-rotating vortices, especially in the trough or crest of the wavy-tapes, were generated by the disturbance of the center-tapered wavy-tape inserts. To verify this flow structures, we carried out the Stereo-PIV (Particle Image Velocimetry) experiments to measure the flow fields. The schematic of the stereoscopic-PIV system is shown in Fig. 20. The experimental system consists of three parts, which are (1) PIV measurement system; (2) water supply; (3) data acquisition and analysis system. The upstream tube allows the flow to be fully developed. In the test section, two cameras take a 45° shooting angle from both sides, and we applied two water prisms to minimize optical deformation of the images. To avoid occlusion, the light sheet generated by laser with lenses is behind the inserts. Before the measurement, we carried out the calibration to ensure the accuracy of the PIV measurement. More details about the experimental setup can refer to our previous works [10,38].

Figs. 21 and 22 shows schematic diagram of the velocity vectors and velocity magnitudes in a circular tube with the center-tapered wavy-tape inserts (A = 5 mm, P = 40 mm, *Re* = 600), respectively. Pairs of counter-rotating vortices were observed at the same position by the PIV measurement. The main characteristics of the flow fields distributions measured by experiment were consistent with that calculated by the numerical methods. Based on the analysis of PIV experimental and numerical results above, the center-tapered wavy-tape inserts could generate longitudinal swirl flow structures in the circular tube and the numerical results had a reasonable reliability.

4.6. Comparison with previous work

In this section, we compare the PEC of the center-tapered wavy-tape insert with that of commonly used inserts such as vortex rod [20], wavy-tape insert [29], helical screw-tape insert [39], and V-baffle [40]. For maintaining a strong mixture with a small disturbance to the core area, as shown in Fig. 23, the PEC of center-tapered wavy-tape insert was better than those of wavy-tape insert, vortex rod, and helical screw-tape insert. The results indicate that the center-tapered wavy-tape insert is a promising tube insert for heat transfer enhancement in practical applications. However, the flow resistance caused by the center-tapered wavy-tape insert is still worth considering. The regularly spaced V-baffle exhibited better PEC. Further investigation will be conducted to improve the overall thermo-hydraulic performance based on the knowledge of the mechanism of the reduction in the flow resistance obtained from the arrangement of V-baffle.

5. Conclusion

A center-tapered wavy-tape insert, with a design inspired by cuttlefish fins, was introduced in this study. For the same Reynolds number and geometric parameters, the comparisons of the thermo-hydraulic performance between smooth tubes with the center-tapered wavy-tape inserts and the conventional wavy-tape inserts were analyzed. The results indicate that the center-tapered wavy-tape inserts had significant effects on the reduction of flow resistance and improvement of overall performance especially when the amplitude was large for laminar flow. This is because the center-tapered wavy-tape insert can produce a similar flow structure and temperature field inside the tube with a small disturbance to the core area. Subsequently, the optimal condition of use of the center-tapered wavy-tape insert was investigated. The larger the waveform factor, the better the heat transfer effects. Considering the practicality of the inserts, the amplitude ratio range was limited—from 0.3 to 0.7. Further, the suitable period ratio was approximately from 2 to 2.5. The best *Nu* was enhanced by 5.23–8.99 times and the best PEC was improved to 2.62. Then, the empirical formulas for *Nu* and *f* were fitted in terms of the waveform factor, period ratio, and the Reynolds number. Finally, the numerical results were verified by the Stereo-PIV experiments. In summary, the center-tapered wavy-tape insert can provide a better overall thermo-hydraulic performance when higher heat transfer and lower flow resistance are required. Therefore, the center-tapered wavy-tape insert is a promising technique for laminar convective heat transfer enhancement.

Acknowledgments

The work was supported by the National Key Research and Development Program of China (No. 2017YFB0603501-3), and the National Natural Science Foundation of China (No. 51776079 and 51736004).

References

[1] J.E. Hesselgreaves, R. Law, D.A. Reay, Compact Heat Exchangers: Selection, Design and Operation, second ed., Butterworth-Heinemann, Kidlington, 2016.
[2] Q. Wang, M. Zeng, T. Ma, X. Du, J. Yang, Recent development and application of several high-efficiency surface heat exchangers for energy conversion and utilization, Appl. Energy 135 (2014) 748–777.
[3] N. Zheng, P. Liu, F. Shan, Z. Liu, W. Liu, Turbulent flow and heat transfer enhancement in a heat exchanger tube fitted with novel discrete inclined grooves, Int. J. Therm. Sci. 111 (2017) 289–300.
[4] N. Zheng, P. Liu, F. Shan, Z. Liu, W. Liu, Heat transfer enhancement in a novel internally grooved tube by generating longitudinal swirl flows with multi-vortexes, Appl. Therm. Eng. 95 (2016) 421–432.
[5] A.E. Bergles, Recent developments in enhanced heat transfer, Heat Mass Transf. 47 (2011) 1001–1008.
[6] M.M. Abu-Khader, An overview on tube inserts configurations and performances in

tubular exchangers, World J. Eng. 13 (2016) 93–108.
[7] H.M. Sandeep, U.C. Arunachala, Solar parabolic trough collectors: a review on heat transfer augmentation techniques, Renew. Sustain. Energy Rev. 69 (2017) 1218–1231.
[8] W.-T. Ji, A.M. Jacobi, Y.-L. He, W.-Q. Tao, Summary and evaluation on single-phase heat transfer enhancement techniques of liquid laminar and turbulent pipe flow, Int. J. Heat Mass Transf. 88 (2015) 735–754.
[9] N. Zheng, P. Liu, F. Shan, Z. Liu, W. Liu, Sensitivity analysis and multi-objective optimization of a heat exchanger tube with conical strip vortex generators, Appl. Therm. Eng. 122 (2017) 642–652.
[10] P. Liu, N. Zheng, F. Shan, Z. Liu, W. Liu, An experimental and numerical study on the laminar heat transfer and flow characteristics of a circular tube fitted with multiple conical strips inserts, Int. J. Heat Mass Transf. 117 (2018) 691–709.
[11] E.Z. Ibrahim, Augmentation of laminar flow and heat transfer in flat tubes by means of helical screw-tape inserts, Energy Convers. Manage. 52 (2011) 250–257.
[12] X. Zhang, Z. Liu, W. Liu, Numerical studies on heat transfer and friction factor characteristics of a tube fitted with helical screw-tape without core-rod inserts, Int. J. Heat Mass Transf. 60 (2013) 490–498.
[13] A. García, P.G. Vicente, A. Viedma, Experimental study of heat transfer enhancement with wire coil inserts in laminar-transition-turbulent regimes at different Prandtl numbers, Int. J. Heat Mass Transf. 48 (2005) 4640–4651.
[14] M.A. Akhavan-Behabadi, R. Kumar, M.R. Salimpour, R. Azimi, Pressure drop and heat transfer augmentation due to coiled wire inserts during laminar flow of oil inside a horizontal tube, Int. J. Therm. Sci. 49 (2010) 373–379.
[15] S. Eiamsa-ard, C. Thianpong, P. Promvonge, Experimental investigation of heat transfer and flow friction in a circular tube fitted with regularly spaced twisted tape elements, Int. Commun. Heat Mass Transf. 33 (2006) 1225–1233.
[16] S. Eiamsa-ard, P. Promvonge, Performance assessment in a heat exchanger tube with alternate clockwise and counter-clockwise twisted-tape inserts, Int. J. Heat Mass Transf. 53 (2010) 1364–1372.
[17] J. Guo, A. Fan, X. Zhang, W. Liu, A numerical study on heat transfer and friction factor characteristics of laminar flow in a circular tube fitted with center-cleared twisted tape, Int. J. Therm. Sci. 50 (2011) 1263–1270.
[18] P. Li, Z. Liu, W. Liu, G. Chen, Numerical study on heat transfer enhancement characteristics of tube inserted with centrally hollow narrow twisted tapes, Int. J. Heat Mass Transf. 88 (2015) 481–491.
[19] L. Syam Sundar, N.T. Ravi Kumar, M.T. Naik, K.V. Sharma, Effect of full length twisted tape inserts on heat transfer and friction factor enhancement with Fe_3O_4 magnetic nanofluid inside a plain tube: An experimental study, Int. J. Heat Mass Transf. 55 (2012) 2761–2768.
[20] N. Zheng, P. Liu, F. Shan, J. Liu, Z. Liu, W. Liu, Numerical studies on thermo-hydraulic characteristics of laminar flow in a heat exchanger tube fitted with vortex rods, Int. J. Therm. Sci. 100 (2016) 448–456.
[21] P. Liu, N. Zheng, F. Shan, Z. Liu, W. Liu, Numerical study on characteristics of heat transfer and friction factor in a circular tube with central slant rods, Int. J. Heat Mass Transf. 99 (2016) 268–282.
[22] N. Zheng, P. Liu, X. Wang, F. Shan, Z. Liu, W. Liu, Numerical simulation and optimization of heat transfer enhancement in a heat exchanger tube fitted with vortex rod inserts, Appl. Therm. Eng. 123 (2017) 471–484.
[23] P. Li, P. Liu, Z. Liu, W. Liu, Experimental and numerical study on the heat transfer and flow performance for the circular tube fitted with drainage inserts, Int. J. Heat Mass Transf. 107 (2017) 686–696.
[24] W. Tu, Y. Wang, Y. Tang, Thermal characteristic of a tube fitted with porous media inserts in the single phase flow, Int. J. Therm. Sci. 110 (2016) 137–145.
[25] W. Tu, Y. Wang, Y. Tang, A numerical study on thermal-hydraulic characteristics of turbulent flow through a circular tube fitted with pipe inserts, Appl. Therm. Eng. 101 (2016) 413–421.
[26] W. Liu, H. Jia, Z.C. Liu, H.S. Fang, K. Yang, The approach of minimum heat consumption and its applications in convective heat transfer optimization, Int. J. Heat Mass Transf. 57 (2013) 389–396.
[27] H. Jia, W. Liu, Z. Liu, Enhancing convective heat transfer based on minimum power consumption principle, Chem. Eng. Sci. 69 (2012) 225–230.
[28] H. Jia, Z.C. Liu, W. Liu, A. Nakayama, Convective heat transfer optimization based on minimum entransy dissipation in the circular tube, Int. J. Heat Mass Transf. 73 (2014) 124–129.
[29] X.W. Zhu, Y.H. Fu, J.Q. Zhao, A novel wavy-tape insert configuration for pipe heat transfer augmentation, Energy Convers. Manage. 127 (2016) 140–148.
[30] Z. Dou, J. Wang, D. Chen, Bionic research on fish scales for drag reduction, J. Bionic Eng. 9 (2012) 457–464.
[31] T. Limei, R. Luquan, H. Zhiwu, Z. Shicun, Experiment about drag reduction of bionic non-smooth surface in low speed wind tunnel, J. Bionic Eng. 2 (2005) 15–24.
[32] Y. Gu, G. Zhao, J. Zheng, Z. Li, W. Liu, F.K. Muhammad, Experimental and numerical investigation on drag reduction of non-smooth bionic jet surface, Ocean Eng. 81 (2014) 50–57.
[33] D.W. Bechert, M. Bruse, W. Hage, R. Meyer, Fluid mechanics of biological surfaces and their technological application, Naturwissenschaften 87 (2000) 157–171.
[34] A. Willy, K.H. Low, Initial experimental investigation of undulating fin, IEEE/RSJ International Conference on Intelligent Robots and Systems, 2005, pp. 1600–1605.
[35] R.L. Webb, Performance evaluation criteria for use of enhanced heat transfer surfaces in heat exchanger design, Int. J. Heat Mass Transf. 24 (1981) 715–726.
[36] P.J. Roache, Perspective: a method for uniform reporting of grid refinement studies, J. Fluids Eng. 116 (1994) 405–413.
[37] F.R. Menter, Ten years of experience with the SST turbulence model, Turbul. Heat Mass Transf. 4 (2003) 625–632.
[38] W. Liu, P. Liu, J.B. Wang, N.B. Zheng, Z.C. Liu, Exergy destruction minimization: a principle to convective heat transfer enhancement, Int. J. Heat Mass Transf. 122 (2018) 11–21.
[39] M.A. Omara, Heat transfer performance through a flat tube using rotary helical screw-tape inserts, Exp. Heat Transf. 29 (2015) 691–706.
[40] W. Jedsadaratanachai, N. Jayranaiwachira, P. Promvonge, 3D numerical study on flow structure and heat transfer in a circular tube with V-baffles, Chin. J. Chem. Eng. 23 (2015) 342–349.